Electronic structure of periodic curved surfaces: Topological band structure

H. Aoki, M. Koshino, D. Takeda,* and H. Morise
Department of Physics, University of Tokyo, Hongo, Tokyo 113-0033, Japan

K. Kuroki
Department of Applied Physics and Chemistry, University of Electro-Communications, Chofu, Tokyo 182-8585, Japan
(Received 6 September 2001; published 11 December 2001)

The electronic band structure for electrons bound on periodic minimal surfaces is differential-geometrically formulated and numerically calculated. We focus on minimal surfaces because they are not only mathematically elegant (with the surface characterized completely in terms of ''navels'') but represent the topology of real systems such as zeolites and negative-curvature fullerenes. The band structure turns out to be primarily determined by the topology of the surface, i.e., how the wave function interferes on a multiply connected surface, so that the bands are little affected by the way in which we confine the electrons on the surface (thin-slab limit or zero thickness from the outset). Another curiosity is that different minimal surfaces connected by the Bonnet transformation (such as Schwarz's *P* and *D* surfaces) possess one-to-one correspondence in their band energies at Brillouin-zone boundaries.

DOI: 10.1103/PhysRevB.65.035102 PACS number(s): 02.40.−k, 73.20.At

I. INTRODUCTION

There is a long history for the fascination with particles bound on curved surfaces, which dates back to the early days of quantum mechanics.[1] There are two complementary points of interest: one is how the particle motions are affected by the local curvature of the surface. The other is how the global topology (i.e., how the surface is wound) affects quantum-mechanical wave functions. The latter problem becomes especially interesting if we consider a *periodic* surface embedded in the three-dimensional space.

Geometrically, Schwarz, back in the 19th century, showed that we can make curved surfaces extend over the entire three-dimensional space by connecting hyperbolic (i.e., everywhere negatively curved) patches. Specifically, Schwarz has constructed *periodic minimal surfaces*, where minimal means that the negatively curved surface has a minimized area with the mean curvature $[\frac{1}{2}(\kappa_1+\kappa_2)$ with κ_1,κ_2 being the principal curvatures] vanishing everywhere on the surface.[2,3]

There are reasons from both condensed-matter physics and mathematics why periodic surfaces are intriguing. First of all, periodic surfaces are of general interest from the perspective of condensed-matter physics. (i) In general, ''crystals'' (periodic structures) composed of surfaces are conceptually interesting as a class of periodic system on which electrons move. Mackay[3-7] has classified them group theoretically (just as the ordinary crystals composed of atoms are classified with the space group), which he named ''flexicrystallography.''

(ii) In terms of materials science, periodic minimal surfaces represent the topology of real condensed-matter systems. These include not only conventional materials such as zeolites or a silica polymorph called melanophlogite,[8,9] or isostructural silicon clathrates,[10] but recent advances in fabrication of exotic materials such as fullerenes or nanotubes have inspired further possibilities such as negative-curvature fullerenes (or a C_{60} zeolite)[7,11–14] whose fabrication has been attempted with a zeolite as a template.[15] Their structures can be modeled as curved surfaces if we smear out atoms into a surface in the effective-mass sense, and it is a fundamental question to consider how a mobile (e.g., π) electron behaves on such surfaces.

Second, there are mathematical interests and simplifications when a periodic surface is minimal: we can exploit the Weierstrass representation, which enables us to specify the surface in a surprisingly simple manner in terms of ''navels.'' The representation also simplifies Schrödinger's equation as we shall show in the present paper.

There are further mathematical fascinations specific to surfaces. One virtue of the structure constructed from surfaces is that we can deform it. One can in fact deform one minimal surface into another with a differential geometrical transformation called the Bonnet transformation. We can then raise a question of how the band structure for one surface could be related to that for the transformed one. Another interest is that some periodic minimal surfaces, such as Schwarz's *P* surface,[16] have a high symmetry (''interior-exterior'' symmetry) that divides the space into two equivalent parts, which should be reflected in the electronic band structure.

So in the present paper we address how the electronic band structures should look like for periodic minimal surfaces. To start with, however, we have to envisage in general two ways (Fig. 1) to confine electrons to a surface: (a) One is to consider electrons bound to a thin, curved slab of thickness d, where the limit $d\rightarrow 0$ is taken.[17] (b) The other is to consider the surface with the degree of freedom normal to the surface ignored from the outset, i.e., a two-dimensional sheet is rolled into the curved surface.[18] Either way it has been shown that an effective potential arises from the curvature of the surface, but that the potential is different between the two cases. Namely, the thin-slab case (a) (Ref. 17) has a potential

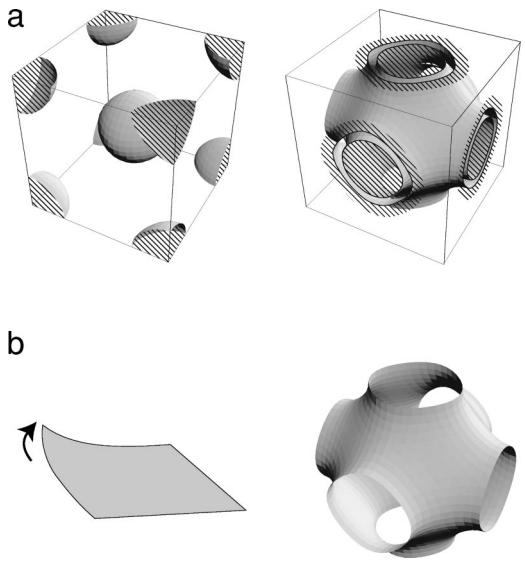

FIG. 1. Two ways to prepare a surface: (a) introduce potential barriers that confine electrons in a three-dimensional space to a thin membrane, or (b) roll a sheet of free electrons into the curved surface.

$$-(\hbar^2/8m)(\kappa_1-\kappa_2)^2,$$

while case (b) (Ref. 18) has

$$+(\hbar^2/8m)(\kappa_1+\kappa_2)^2.$$

The origin of the discrepancy was subsequently revealed by Ikegami and coworkers:[19] when the degree of freedom normal to the surface is ignored, Dirac's prescription for constrained systems can be applied, but there is room for ambiguity in the order of operators. If we adopt the conservation constraint, the resultant equation reduces to that in the $d \to 0$ approach. When the surface is minimal ($\kappa_1+\kappa_2=0$), the curvature potential is nonzero in general (since $\kappa_1-\kappa_2 = 2\kappa_1 \neq 0$) in case (a), while the curvature potential vanishes identically in (b).

For condensed-matter systems such as atoms arrayed along a curved surface, we should take the $d \to 0$ approach. Still, the difference in the band structure between the two cases is curious. Namely, although we have a periodic system in either case, the periodicity imposed in case (a) is the periodicity in the strong potential that confines the electron into a thin slab [Fig. 1(a)], while in case (b) the electron moves freely along the surface, where the only constraint is that an electron has to move in a space having a nontrivial topology. The topology can have a profound effect on the electron's wave function, since, if we regard the periodic surface as a network of pipes (a cubic network for the *P* surface, diamond for the *D* surface, etc.), the wave function interferes with itself along various paths wound around the ''necks.'' Thus the periodicity felt by an electron amounts to the strong confining potential in case (a), while the periodicity only enters as a way in which the wave function interferes in case (b), and it is an intriguing question whether or not their band structures are similar.

The purpose of this paper is (i) to explicitly write Schrödinger's equation for electrons on periodic minimal surfaces by exploiting Weierstrass's representation in order to obtain the electronic band structure and (ii) to calculate and compare the band structures in cases (a) and (b). Unexpectedly the band structures turns out to be similar between cases (a) and (b), i.e., the bands are primarily determined from the topological way in which the wave function interferes with itself. The energy scale of the band structure (band splitting, such as a split of the ''*d*'' band into E_g and T_{2g}, and bandwidths) is also universally $\sim\hbar^2/2mL^2$ with L being the linear dimension of the unit cell of the periodic surface. (iii) We go further to ''Martensitic-deform'' a surface to another connected by the Bonnet transformation. We shall show that there exists a curious one-to-one correspondence in their band structures, which illustrates another unique feature in the topological band structure.

II. WEIERSTRASS REPRESENTATION OF MINIMAL SURFACES

We start with a mathematical prerequisite for representing minimal surfaces. A two-dimensional surface $\mathbf{r}(q^1,q^2)$ embedded in a three-dimensional space can be expressed in terms of two-dimensional coordinates q^1,q^2, where $(q^1,q^2) \equiv (u,v)$ are called isothermal when the metric tensor g_{ij} is diagonal with

$$d\mathbf{r}\cdot d\mathbf{r} = g_{11}(du\,du + dv\,dv).$$

What Weierstrass and Enneper have found is that a necessary and sufficient condition for $\mathbf{r}(u,v)$ representing a minimal surface with isothermal $(u,v) \in S$ (S: a simply connected region) is that there exist F,G, functions of $w \equiv u+iv$, with which $\mathbf{r}(u,v)=[x(u,v),y(u,v),z(u,v)]$ is expressed as

$$\mathbf{r}(u,v) = \mathrm{Re}\left(\int_{w_0}^{w} F(1-G^2)dw, \times \int_{w_0}^{w} iF(1+G^2)dw, \int_{w_0}^{w} 2FG\,dw \right), \qquad (1)$$

where w_0 is a constant, and FG^2 is assumed to be regular (i.e., mth poles of G assumed to coincide with $2m$th zeros of F).[4,5,20] If there are singularities that violate this condition, we can exclude these points by incising cut(s) to make S a Riemann surface. Thus there is a one-to-one correspondence between a minimal surface and the functional form of F,G.

Now, Schrödinger's equation for a curved surface, expressed with two-dimensional coordinates (q^1,q^2) and metric tensor g_{ij}, is written as

$$\left[-\frac{\hbar^2}{2m}\frac{1}{\sqrt{g}}\frac{\partial}{\partial q^i}\sqrt{g}g^{ij}\frac{\partial}{\partial q^j} - \frac{\hbar^2}{8m}(\kappa_1-\kappa_2)^2 \right]\psi(q^1,q^2) = E\psi(q^1,q^2), \qquad (2)$$

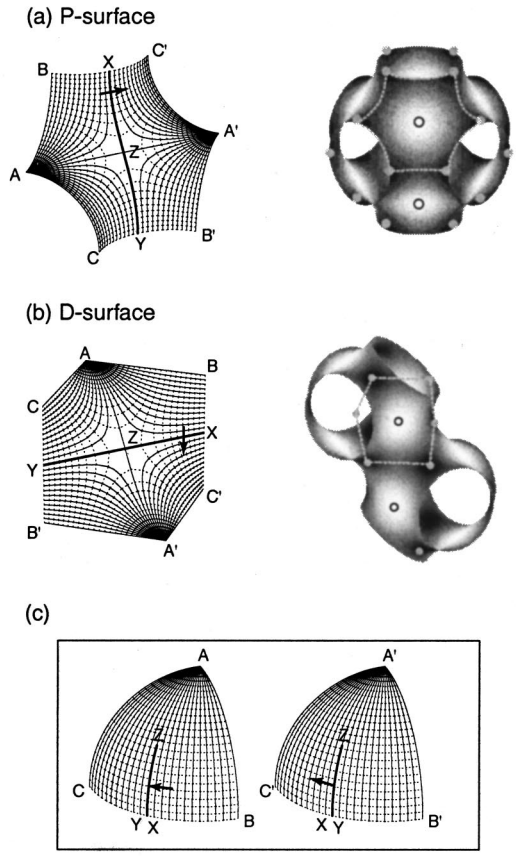

FIG. 2. The structures of P (a) and D (b) surfaces. We show a unit patch on the left panel, and a full unit cell on the right. The gray scale in the right panel represents the curvature potential, where shaded (open) circles depict potential minima (maxima, coinciding with the navels). (c) The stereographic projection from the minimal surface to Gauss spheres. A unit patch of P or D corresponds to a pair of 1/8 spheres.

where summations over repeated indices are assumed. This equation is for model (a), while we can replace the second term in the bracket (potential term) by $+(\hbar^2/8m)(\kappa_1+\kappa_2)^2$ for model (b).

In the Weierstrass-Enneper representation, every quantity in Schrödinger's equation can be expressed in terms of F and G, since the Laplacian, the first term in the angular brackets in Eq. (2), reduces to $(\partial^2/\partial q_i^2)/\sqrt{g}$ in the isothermal coordinates, where

$$g \equiv \det\{g_{ij}\} = \left[\frac{1}{2}|F|(|G|^2+1)\right]^4,$$

while we can plug in $\kappa_1 = -\kappa_2 = 4|G'|/|F|(|G|^2+1)^2$ for the curvature term. Schrödinger's equation for periodic minimal surfaces then reduces to

$$-\frac{4}{|F|^2(|G|^2+1)^2}\left[\frac{\partial^2}{\partial u^2}+\frac{\partial^2}{\partial v^2}+\frac{4|G'|^2}{(|G|^2+1)^2}\right]\psi = \varepsilon\psi, \tag{3}$$

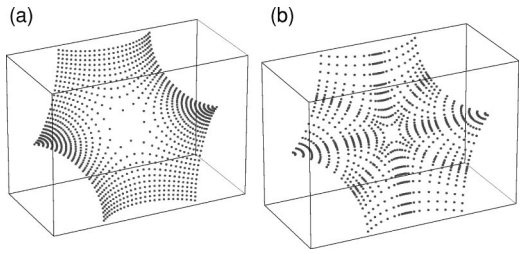

FIG. 3. Descretization for the spherical coordinates: (a) a mesh with even intervals in θ and ϕ and (b) uneven ones, adopted here, which take care of the singular point in the Jacobian.

where $\varepsilon \equiv E/(\hbar^2/2m)$. As evident from the Weierstrass representation (1), F has the dimension of length and G is dimensionless. Hence the energies in minimal surfaces always scale as $E/(\hbar^2/2mL^2)$, where $L \sim F \sim$ linear dimension of the unit cell [a precise expression given in Eq. (5) below].

We can have a more transparent form when $G(w)=w$ (as is often the case with periodic minimal surfaces, including the P surface). In this case we can exploit the stereographic map (Gauss map) from the infinite complex plane (u,v) to a unit sphere (θ,ϕ),

$$w = u + iv = \cot\left(\frac{\theta}{2}\right)e^{i\phi}.$$

After a bit of algebra, we finally arrive at the differential equation for (θ,ϕ),

$$-\frac{(1-\cos\theta)^4}{|F|^2}\left(\frac{\partial^2}{\partial\theta^2}+\cot\theta\frac{\partial}{\partial\theta}+\frac{1}{\sin^2\theta}\frac{\partial^2}{\partial\phi^2}+1\right)\psi = \varepsilon\psi. \tag{4}$$

Curiously, a common coefficient $(1-\cos\theta)^4/|F|^2$ factors out for the Laplacian (the first three terms in the large parentheses in the above equation) and the curvature potential $(+1)$, which is made manifest due to the Weierstrass representation. Hence the kinetic and potential energies vary in a correlated manner as we go from one minimal surface to

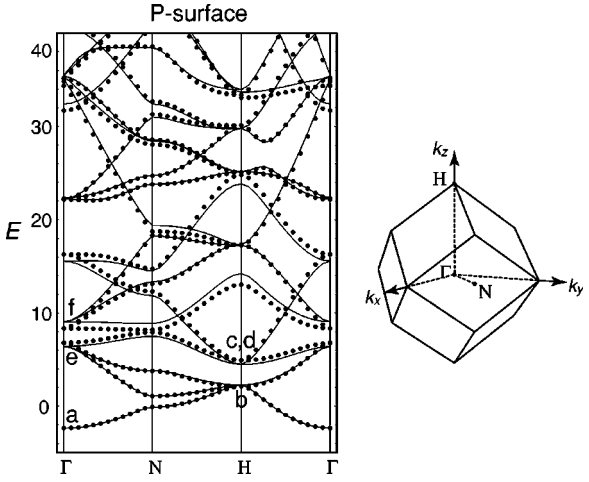

FIG. 4. The energy-band structure in units of $\hbar^2/2mL^2$ is shown for the P surface, when the curvature potential is considered (curves) or ignored (dots) with an energy offset to make the band bottoms coincide between the two cases. The inset depicts the Brillouin zone for a bcc unit cell.

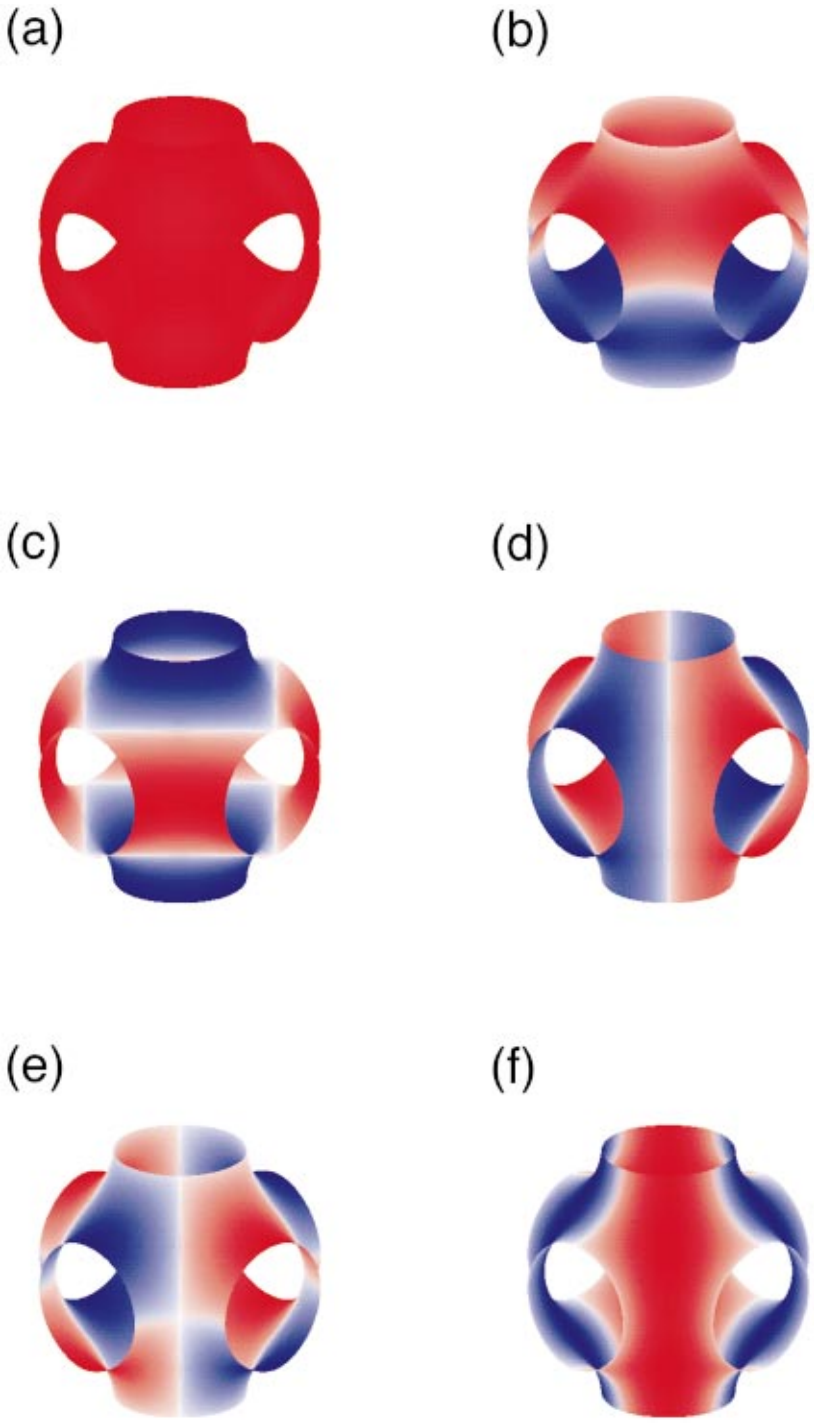

FIG. 5. (Color) Typical wave functions for a unit cell of *P* surfaces with positive (negative) amplitudes color coded in red (blue). Their eigenenergies are indicated in Fig. 4.

another by changing *F*. However, this does not imply that the curvature potential always exerts as large an effect as the kinetic energy does, since the expectation values of the kinetic and potential energies depend on the amplitude of the wave function, and a quantitative study is required.

III. RESULTS FOR SCHWARZ'S *P* SURFACE

So we first take Schwarz's *P* surface as a typical triply periodic (periodic in x,y,z) minimal surface, or a ''simple cubic'' minimal surface (belonging to space group $Im3m$ in the language of flexicrystallography). Some authors[20–22] gave the Weierstrass-Enneper representation for the *P* surface as

$$F(w)=iL/\sqrt{1-14w^4+w^8}, \tag{5}$$

where $L\sim$ linear dimension of the unit cell (to be precise the unit-cell size is $2.157L$, which is given as an elliptic integral).

A unit cell of the *P* surface comprises eight identical patches, as shown in Fig. 2. With the stereographic mapping discussed above, a unit cell is mapped onto two spheres,

connected into a Riemann surface via four cuts, which have to be introduced to make FG^2 nonsingular since F has poles.

Differential geometrically F is in general specified solely by such poles in a form $F \propto 1/\Pi_i (w-w_i)^\eta$ where η determines the topology of the surface. In fact the poles correspond, in the language of differential geometry, to the *navels* (umbilical points), which are defined as the points where every cross section is inflected, with the two principal curvatures becoming degenerate, $\kappa_1 = \kappa_2$ ($=0$ for a minimal surface). So a periodic minimal surface is completely characterized by the navels that appear periodically. The curvature potential $\propto -(\kappa_1 - \kappa_2)^2$ in case (a) varies on the surface, which may be called a ''crystal field'' in flexicrystals. Navels then specify the positions where the curvature potential becomes maxima ($=0$), while the minima occurs at the maxima of the absolute value of κ_1 ($=-\kappa_2$ for a minimal surface). In the P surface the navels (potential maxima) occur at eight ''Affensattel'' (monkey's-saddle) points in a unit cell,[23,21] while the potential minima occur at four points around each nape of the neck as depicted in Fig. 2(a).[24]

IV. RESULTS FOR THE BAND STRUCTURE

A. Band structure for case (a)

In Schrödinger's equation for periodic minimal surfaces, Eq. (4), the variables θ, ϕ cannot be separated, so that we have solved the equation numerically by discretizing θ, ϕ to diagonalize the Hamiltonian matrix. In discretizing the spherical coordinates, special care is taken around the navels, since the Jacobian J of the transformation to the Gauss sphere is singular there (Fig. 3). The band structure is obtained by connecting the adjacent unit cells with appropriate phase factors.

We now come to the result for the band structure for the P surface in Fig. 4 (curves), and typical wave functions at Γ and H in the bcc Brillouin zone (Γ in the simple cubic zone) in Fig. 5. The P surface happens to divide the space into two equivalent parts, since a body center enclosed by the surrounding unit cells has the same shape as the original unit, so that we first note that the true symmetry is body-centered cubic rather than simple cubic. So the bands are displayed on the Brillouin zone for bcc. In accord with the above argument, the energy scale (bandwidth, splitting, etc.) is $\sim \hbar^2/2mL^2$. This is of the order of 1 eV for $L \sim 10$ Å, the unit-cell size assumed for a hypothetical negative-curvature fullerene.[25]

The curvature, or the effective mass, of these bands are either positive (electronlike) or negative (holelike) according to the nature of the wave function. The mass cannot be estimated with a simple $\mathbf{k}\cdot\mathbf{p}$ perturbation, since the perturbation $\propto \mathbf{k}\cdot\mathbf{p}$ derives from the fact that the Hamiltonian $H_0 \propto \mathbf{p}^2$ while H_0 has no such simple form on a curved surface. In other words, the $\mathbf{k}\cdot\mathbf{p}$ formula has $\Sigma_j (\langle i|p_\mu|j\rangle\langle j|p_\nu|i\rangle)/(E_i - E_j)$, so we would have to calculate the matrix elements of $\mathbf{p}$ for wave functions that are finite only along the surface.

B. Band structure for case (b)

Now we are in position to compare the (a) confinement case (curves in Fig. 4) with the (b) rolled case (dotted lines in Fig. 4). We can immediately see that the two band structures are rather similar up to some offset ($2.34\hbar^2/2mL^2$). This is surprising, since there is no *a priori* reason why they should be. To be more precise, quantitative features characterizing the band, i.e., the effective mass and bandwidths, are similar between the two cases. So we conclude that the band structure does not essentially depend on the way in which electrons are confined, at least for ''gently'' curved surfaces such as minimal surfaces where there are no sharp edges that would give large curvature potentials.

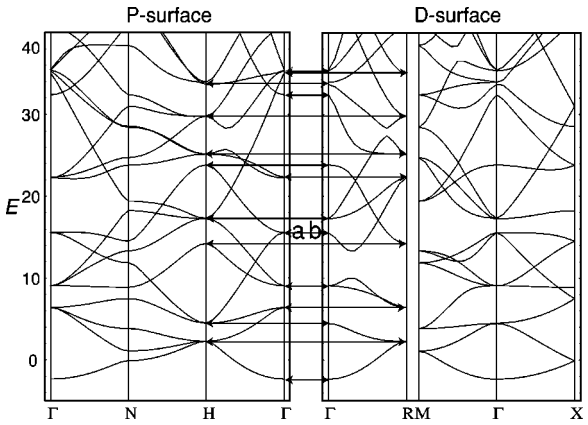

FIG. 6. The band structures for the P and D surfaces. Horizontal lines indicate how the energies at the zone center or edges coincide between the two cases.

V. BONNET TRANSFORMATION

A. Bonnet transformation

The next important question is whether the band structures for surfaces connected by the Bonnet transformation are related.

The deformation of the P surface to other periodic minimal surfaces can be implemented by the Bonnet transformation, which is conformal and is represented by an elliptic transformation. A beautiful asset of the Weierstrass representation for minimal surfaces is that the Bonnet transformation is simply represented by a phase factor, $F \rightarrow Fe^{i\beta}$, in Eq. (1), where β is called the Bonnet angle. If we apply this to the P surface (cubic), the transformation changes[20] it into the G surface (gyroid with $\beta = 0.211\pi$) and the D surface (diamond with $\beta = \pi/2$), which may be regarded as a ''Martensitic transformation'' in the words of Ref. 26. The structure of the D surface is depicted, along with the P surface, in Fig. 2. Since the D surface has a diamond symmetry, its unit cell contains two ''cages.''

We can first note that the Bonnet transformation preserves the metric tensor and the Gaussian curvature. This implies that all the surfaces connected by the Bonnet transformation obey the *identical* Schrödinger equation within a unit patch. Indeed, if we look at Schrödinger's Eq. (4), F only enters as $|F|$, so that $F \rightarrow Fe^{i\beta}$ does not alter the equation. Although this is curious enough, this does not mean that the band structures are identical, since, while the transformed surfaces share the same genus (= three for P and D), the way in which unit cells are connected is different among them.

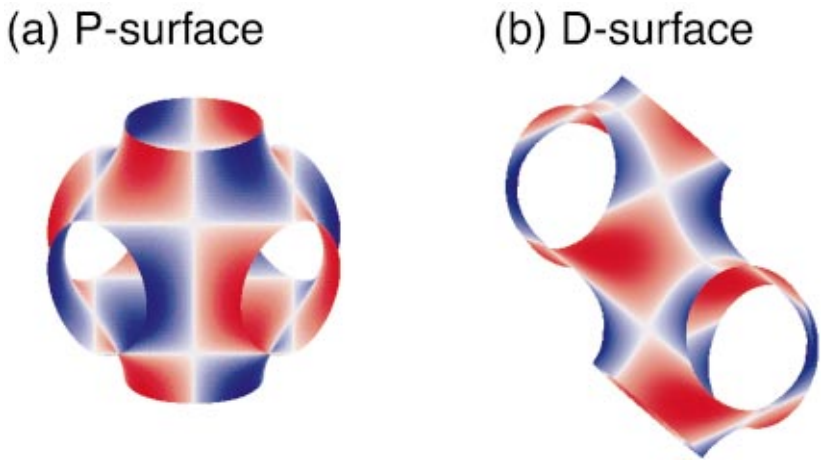

FIG. 7. (Color) Typical wave functions for a unit cell of the Bonnet-connected *P* and *D* surfaces with positive (negative) amplitudes color coded in red (blue). Their eigenenergies are indicated in Fig. 6.

B. Band structure of a Bonnet-transformed surface

Figure 6 compares the band structures for the *P* and *D* surfaces. The two band structures are indeed different due to the difference in the three-dimensional connection of the unit cells discussed above. Curiously, however, we find that the values of the band energy at *special points* (Brillouin-zone corners, edges, and face centers) have identical sets of values between different surfaces. Namely, a close comparison of the two band structures reveals that the band energies exactly coincide, where the ''law of correspondence'' is

P surface		*D* surface
Γ, H	$\Leftrightarrow$	Γ, R
N	$\Leftrightarrow$	X, M.

This can be explained from the property of the Bonnet transformation that does not change Schrödinger's equation. For this purpose we have to look at the unit cells more closely. In Fig. 8, we show how unit patches are connected for the *D* and *P* surfaces. We have indicated in the figure how the eight patches in a unit cell, numbered with 1 through 8, are connected to other patches in the adjacent cells by marking the edges with those numbers (i.e., if an edge is marked with, say, 7, the adjacent patch should be 7). The wave function should be continued to the adjacent patch with a certain phase factor. We have indicated the connection coefficients,

$$\rho_i = \exp(i\phi_i),$$

where ϕ_i is the Bloch phase along $i=x,y,z$. Hence this diagram fully characterizes how the Bloch wave functions are connected on the periodic minimal surfaces in terms of patches. We can then compare the coefficients for the *P* and *D* surfaces to extract a correspondence at special points in *k* space.

In the diagrams introduced here naturally different patch numbers are assigned to them between the *P* and *D* surfaces, since the way in which the patches are connected (i.e., numbers attached to the edges) is different between them. However, we can make them identical, if we rearrange the connection numbers by noting the symmetry. Since the parity

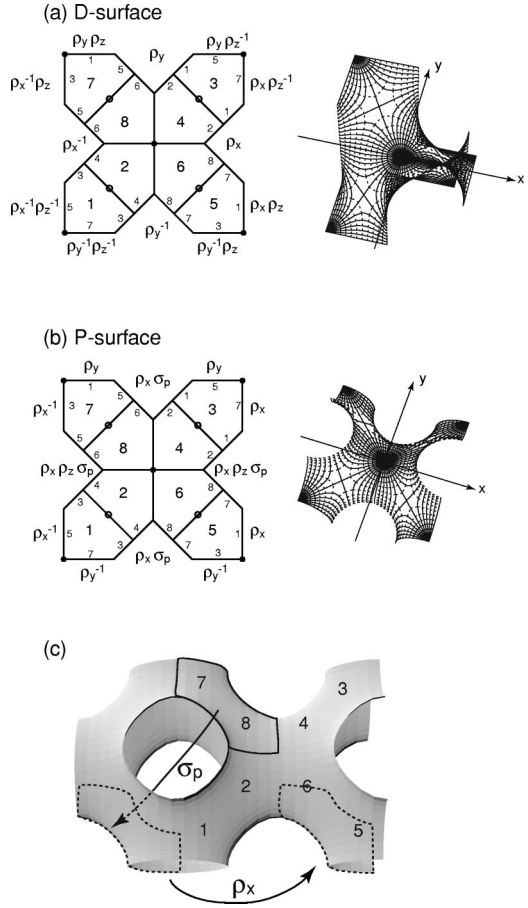

FIG. 8. (a) The way in which patches (labeled by large numbers) are connected to those in adjacent unit cells are indicated by small numbers attached to the edges for the *D* surface. The Bloch phase factors (ρ_i's) are also shown. In the left panels the patches are flattened and expanded, while the right panels depict the actual three-dimensional shapes. (b) The corresponding diagram for the *P* surface, where we have rearranged the numbers to make them identical with those for the *D* surface by exploiting the symmetry. Accordingly the Bloch phase factors for the *P* surface involve the parity inversion (σ_p). An example is shown in (c), which indicates how patches 7,8 are neighboring 5,6 through $\rho_x\sigma_p$.

inversion σ_p with respect to the center of a unit cell preserves the Hamiltonian and does not change the special k vectors on the zone edges either, the group theory dictates that the eigenstates on those k points should have the parity 1 or -1. Then we can always construct the wave function for one half of the unit cell by multiplying the wave function for the other with 1 or -1. Namely, if we employ a simple cubic unit cell for the P surface [Fig. 2(a), right panel which is twice the bcc unit cell depicted in Fig. 8(b)] to make the correspondence clearer, we can reproduce the wave function in the lower half from that in the upper half by applying σ_p, which enables us to make the connection numbers in P the same as in D as shown in Fig. 8. So we have now the same connection numbers between P and D, where the only difference is different connection coefficients (ρ_i's) between P and D as indicated in the figure. If we compare these, we end up with a ''law of corresponding k points,''

P surface k points (ρ_x,ρ_y,ρ_z)			D surface k points (ρ_x,ρ_y,ρ_z)
$\Gamma(1,1,1)$	$\sigma_p=1$	$\Leftrightarrow$	$\Gamma(1,1,1)$
	$\sigma_p=-1$	$\Leftrightarrow$	$R(-1,-1,-1)$
$M(-1,-1,1)$	$\sigma_p=-1$	$\Leftrightarrow$	$X(1,1,-1)$
	$\sigma_p=1$	$\Leftrightarrow$	$M(-1,-1,1)$

We can immediately translate this into the correspondence found above, $\Gamma,H\Leftrightarrow\Gamma,R$, etc., if we note the relation,

simple cubic		bcc
Γ	$\Leftrightarrow$	Γ, H
M	$\Leftrightarrow$	N

between the simple cubic and bcc unit cells.

The wave functions shown in Fig. 7 are actually related through this relation. A simplest way to confirm this is to note that the wave function on each unit patch behaves in a similar manner. In fact, the wave function $\psi(\theta,\phi)$ in Eq. (4) is identical between the two surfaces.

VI. DISCUSSION

The band structures revealed here should have important implications for various physical properties. These should include transport properties as well as the cyclotron resonance, which can detect the effective mass arising from topological band structures. Since the mass is determined by the interference of wave functions, effects of external magnetic fields should also be interesting.

We can finally comment that if we adopt foams of graphite to realize curved surfaces,[7] then the equation of motion of π electrons on the network of the honeycomb lattice will become, in the effective-mass picture, the problem of a zero-mass Dirac equation (i.e., Weyl's equation) on curved surfaces. While we have ignored spin degrees of freedom here, the spin connection on the surface will give rise to a Berry's geometrical phase.

ACKNOWLEDGMENTS

H.A. wishes to thank Alan Mackay for illuminating correspondences, Hiroshi Kuratsuji and Koichi Fukuda for discussions, and Yasuo Nozue for pointing out Ref. 15.

*Present address: SGI Japan, Ltd., Ebisu, Shibuya, Tokyo 150-6031, Japan.

[1] B.S. DeWitt, Rev. Mod. Phys. **29**, 377 (1957).
[2] See, e.g., S. Kobayashi and K. Nomizu, *Foundations of Differential Geometry* (Wiley, New York, 1969).
[3] A.L. Mackay, Nature (London) **314**, 604 (1985).
[4] H. Terrones and A. L. Mackay, in *Growth Patterns in Physical Sciences and Biology*, edited by J. M. Garcia-Ruiz, E. Louis, P. Meakin, and L. M. Sander (Plenum, New York, 1993), p. 315.
[5] A. Mackay, Curr. Sci. **69**, 151 (1995).
[6] O.D. Friedrichs, A.W.M. Dress, D.H. Huson, J. Klinowski, and A. L. MacKay, Nature (London) **400**, 644 (1999).
[7] A.L. Mackay and H. Terrones, Nature (London) **352**, 762 (1991).
[8] S. Tsuneyuki, H. Aoki, and Y. Matsui, in *Computer Aided Innovation of New Materials*, edited by M. Doyama, T. Suzuki, J. Kihara, and R. Yamamoto (Elsevier, New York, 1991), p. 381.
[9] *Physics Meets Mineralogy—Condensed-Matter Physics in Geosciences*, edited by H. Aoki, Y. Syono, and R. J. Hemley (Cambridge University Press, Cambridge, England, 2000).
[10] K. Moriguchi, M. Yonemura, A. Shintani, and S. Yamanaka, Phys. Rev. B **61**, 9859 (2000), and references therein.
[11] D. Vanderbilt and H. Tersoff, Phys. Rev. Lett. **68**, 511 (1992).
[12] M. O'Keeffe, Phys. Rev. Lett. **68**, 2325 (1992).
[13] T. Lenosky, X. Gonze, M. Teter, and V. Elser, Nature (London) **355**, 333 (1992).
[14] This kind of structure has been generalized into what M. Fujita, T. Umeda, and M. Yoshida [Phys. Rev. B **51**, 13 778 (1995)] called ''Pearcene'' after the architect Peter Pearce.
[15] T. Kyotani, T. Nagai, S. Inoue, and A. Tomita, Chem. Mater. **1997**, 609 (1997).
[16] H.A. Schwarz, *Gesammelte Mathematische Abhandlungen* (Springer, Berlin, 1890).
[17] M. Ikegami and Y. Nagaoka, Prog. Theor. Phys. Suppl. **106**, 235 (1991).
[18] N. Ogawa, K. Fujii, and A. Kobushukin, Prog. Theor. Phys. **83**, 894 (1990).
[19] M. Ikegami, Y. Nagaoka, S. Takagi, and T. Tanzawa, Prog. Theor. Phys. **88**, 229 (1992).
[20] H. Terrones, J. Phys. Colloq. **51**, 345 (1990).
[21] D. Cvijović and J. Klinowski, J. Phys. I **2**, 2191 (1992).
[22] J. Klinowski, A.L. Mackay, and H. Terrones, Philos. Trans. R. Soc. London, Ser. A **354**, 1975 (1996).
[23] D. Hilbert and S. Cohn-Vossen, *Anschauliche Geometrie* (Springer, Berlin, 1932), Sec. 28.
[24] If we mimic such structures with a graphite foam (i.e., a membrane of a mostly hexagonal lattice), the potential minima cor-

respond to the positions of eight-membered rings (introduced to make the curvature negative) (Refs. 4, 7, and 25).

[25] S.J. Townsend, T.J. Lenosky, D.A. Muller, C.S. Nichols, and V. Elser, Phys. Rev. Lett. **69**, 921 (1992).

[26] S.T. Hyde and S. Andersson, Z. Kristallogr. **174**, 225 (1986). However, we cannot actually change the Bonnet angle continuously, since the surface does not close but intersects with itself for the angles between these values.